

The bark biorefinery: a side-stream of the forest industry converted into nanocomposites with high oxygen-barrier properties

Myriam Le Normand · Rosana Moriana ·
Monica Ek

Received: 6 May 2014 / Accepted: 30 August 2014 / Published online: 6 September 2014
© Springer Science+Business Media Dordrecht 2014

Abstract The purpose of the bark biorefinery concept is to upgrade the different constituents present in bark to multiple value-added bio-based products. Non-cellulosic polysaccharides (NCP) and cellulose nanocrystals (CNC) sequentially isolated from the inner bark of Norway spruce were used as raw materials for the formulation of renewable nanocomposites. The film formation abilities of NCP/CNC formulations prepared with different proportions of CNC were studied. Homogeneous transparent films with a glossy appearance were obtained when more than 30 wt% CNC was incorporated. The influence of the CNC content on the NCP/CNC films was assessed in terms of structural, thermal, mechanical and oxygen-barrier properties. All the films showed better performances with increasing CNC content, which was explained by the strong interactions between the two components. The effect on the film performances of adding sorbitol as a plasticizer was also evaluated. The presence of sorbitol decreased the thermal stability, the stiffness and the oxygen permeability of the films at 80 % RH.

Electronic supplementary material The online version of this article (doi:[10.1007/s10570-014-0423-z](https://doi.org/10.1007/s10570-014-0423-z)) contains supplementary material, which is available to authorized users.

M. Le Normand · R. Moriana · M. Ek (✉)
Division of Wood Chemistry and Pulp Technology,
School of Chemical Science and Engineering, KTH Royal
Institute of Technology, Teknikringen 56,
10044 Stockholm, Sweden
e-mail: monicaek@kth.se

However, the addition of sorbitol enhanced the elongation of the films and further improved their oxygen-barrier properties at 50 % RH. The composite properties could thus be tailored by adding different amounts of sorbitol and CNC, resulting in all-carbohydrate materials with performances similar to or even better than the conventional barrier materials used in packaging.

Keywords Bark · Biorefinery · Cellulose nanocrystals · Nanocomposites · Oxygen-barrier · Pectins

Introduction

The forest biorefinery concept is a strategic approach in line with present concerns relating to sustainability and the adverse ecological footprint of petroleum-based fuels and polymeric materials. The upgrading of lignocellulosic biomasses into biochemicals and biodegradable packaging could be a way of decreasing the carbon footprint and increasing the profitability of the pulp, paper and packaging industries (Shen and Patel 2008).

Norway spruce (*Picea abies*) is a predominant softwood species in the European forest and is intensively used in the pulp and paper industry (Bertaud and Holmbom 2004). The bark of Norway spruce is a major byproduct of the pulp and paper

ills, and it is usually burnt for energy production. In addition to its fuel value and thanks to its unique chemical composition, this bark could also be a rich source of high-value chemicals. In this sense, a bark biorefinery that first extracts valuable compounds such as extractives (Co et al. 2012; Nilsson et al. 2011; Pietarinen et al. 2006), tannins (Kempainen et al. 2014; Pizzi 2006), non-cellulosic polysaccharides (NCP) (Le Normand et al. 2012, 2014a) and cellulose (Le Normand et al. 2014b), and thereafter converts the residue into biofuels and energy could be interesting (Ragauskas et al. 2006).

The major constituents of the bark of Norway spruce are polysaccharides. Altogether, hemicelluloses, pectins and cellulose constitute about 50 % of the inner bark, 33 % of the outer bark (Krogell et al. 2012) and 40 % of the whole bark collected immediately after the debarking process in a pulp mill (Le Normand et al. 2012; Miranda et al. 2012). Recently, we showed that the recovery of the NCP from the bark of Norway spruce was possible through a series of hot-water extractions and filtration steps (Le Normand et al. 2012, 2014a). The crude NCP extract contained mainly pectin and starch as well as a minor amount of Klason lignin. The purpose of later studies was to find direct applications for the crude bark polysaccharide mixture, avoiding time-consuming and costly refining steps. One example of such an application was described in a previous work and presented bark hot-water extracts as potential immunostimulating agents (Le Normand et al. 2014a).

Another straightforward way of adding value to a polysaccharide mixture, without further refining, is to produce functional biomaterials. This approach was first reported for polysaccharide mixtures obtained from thermomechanical pulping (Hartman et al. 2006) and wood hydrolysates (Edlund et al. 2010; Ryberg et al. 2011). The authors showed that wood polysaccharide mixtures in the least upgraded state were able to give films with an even better performance in terms of oxygen permeability (OP) than corresponding films based on highly purified hemicellulose (Ibn Yaich et al. 2011). Mikkonen et al. (2010b) reported the same kind of synergic effect with spruce galactoglucomannan and Konjac glucomannan which had a better oxygen-barrier property when used as a blend than films from either of the raw materials alone.

However, hemicellulose-based films often suffer from poor mechanical properties which restrict their

use for many applications. One technique to increase the mechanical strength of a polysaccharide film is to form a composite with another polysaccharide that can create strong interactions (Dufresne 2008; Moriana et al. 2011). In recent years, the incorporation of biodegradable nanofillers such as cellulose nanocrystals (CNCs) into a polymer matrix has been shown to be an important strategy for obtaining nanocomposites with a high mechanical performance (Mariano et al. 2014). Recently, we reported the isolation of CNCs from the inner bark residue of Norway spruce after the extraction of NCP (Le Normand et al. 2014b). Bark CNCs had a high aspect ratio ($l/d = 63$), high crystallinity index (CI) (84 %) and good thermal stability which make them an excellent candidate for use as reinforcing agents in nanocomposites. Compared to inorganic reinforcing fillers, CNCs have advantages such as positive ecological footprint, low density and ease of recycling. CNCs can be added to hemicellulose-based films, not only to reach better mechanical properties, but also to lower the OP (Mikkonen et al. 2010b; Saxena et al. 2010). Low OP as well as mechanical strength and flexibility can be important target properties for applications such as packaging films (Hansen and Plackett 2008).

Our aim was to produce films with good mechanical, thermal and oxygen-barrier properties based essentially on spruce bark polysaccharides. Films were prepared from the partially upgraded NCP fraction obtained after hot-water extraction of the inner bark of Norway spruce in combination with CNCs isolated from the same raw material. The effect of the addition of sorbitol as a plasticizer was also evaluated.

Materials and methods

Materials

Bark of Norway spruce was taken from a fresh 30-year-old tree cut in Gävleborg County (Sweden) in July 2009 and stored in the dark at -20°C . The inner and outer bark were separated manually using a scalpel. The inner bark was ground with a hand blender to a particle size of approximately 5×2 mm. The ground inner bark was extracted with an Accelerated Solvent Extractor at 140°C (ASE) (Dionex, California) following the method described by Le Normand et al. (2012).

The product obtained after hot-water extraction at 140 °C, contained mainly pectin and starch carbohydrates (64 and 14 %, respectively), for this reason this product was designed as NCP (Le Normand et al. 2014a). However, the hot-water extracts also contained 4 % of lignin, 1 % of ash and some minor amounts of mannose and xylose in their formulation. The average molecular weights were Mn = 15 kDa and Mw = 55 kDa. The detailed extraction procedure as well as the carbohydrate composition and linkage analyses of the NCP fraction was reported in a previous study (Le Normand et al. 2014a).

The residue after extraction of NCP at 140 °C was freeze-dried and used for the isolation of CNCs. The isolation process and CNC characterization have recently been reported (Le Normand et al. 2014b). Briefly, the residue was bleached with sodium chlorite and hydrolyzed in sulfuric acid (60 % w/w) at 50 °C for 60 min. The CNCs had rod-like aspects with a diameter and length of the order of 2.8 and 175 nm, respectively, giving an aspect ratio >60.

Analytical grade chemicals used for extraction, bleaching, hydrolysis and carbohydrate analysis were purchased from Sigma-Aldrich and used without further purification.

Preparation of NCP/CNC formulations

The freeze-dried NCP powder and CNC water-based suspension were mixed together at room temperature until a homogeneous dispersion was obtained with a CNC content of 10, 20, 30, 40, 50 wt%. These formulations were coded as CNC10, CNC20, CNC30, CNC40 and CNC50. When sorbitol was added, its content was fixed at 30 % on the basis of the dry NCP weight. The samples were then coded CNC30S, CNC40S and CNC50S. Films were obtained by casting in polystyrene petri dishes and drying in an oven at 40 °C for 65 h. Sample thicknesses were determined with a Mitutoyo micrometer by taking the average of five independent measurements. The thickness of the films varied between 17 and 22 μm, depending on the CNC content.

Atomic force microscopy (AFM)

The morphology of the formulations was imaged in the dry state with tapping-mode AFM (Multimode V, Bruker, Santa Barbara, CA). Images phase modes

were recorded with an E-scanner. TAP150 silica cantilevers (Bruker) having a tip with a nominal radius of 8 nm and a spring constant of 5 N/m oscillated at its fundamental resonance frequencies between 150 and 200 kHz.

Fourier transform infrared spectrometry (FTIR)

Fourier transform infrared spectrometry (FTIR) was carried out on a Perkin–Elmer Spectrum 2000 FTIR with an attenuated total reflectance (ATR) crystal accessory (Golden Gate). Spectra of the CNC, NCP and NCP/CNC composites were obtained as 16 individual scans at 2 cm⁻¹ resolution in the 4,000–600 cm⁻¹ interval. All spectra were smoothed and fitted to an automatic base line correction by OMNIC 7.0 software.

Wide angle X-ray scattering (WAXS)

The CNC, NCP and NCP/CNC formulations were studied at ambient temperature in an X-ray diffractometer (X’Pert PRO MPD PANalytical, The Netherlands) using a monochromatic CuKα radiation ($\lambda = 1.54 \text{ \AA}$) in the range of $2\theta = 10\text{--}50^\circ$ with a scanning rate of 1.0° min⁻¹. X-ray diffraction data were processed and analyzed using HighScore Plus 3.0 software (PANalytical, Inc.). The CI of the formulations was determined using the peak height method and calculated by the Segal empirical method (Segal et al. 1959) after subtraction of the background signal:

$$\text{CI} (\%) = \frac{(I_{200} - I_{AM})}{I_{200}} \times 100$$

where I_{200} is the peak intensity (200) corresponding to crystalline cellulose I at 2θ of 22.5°, and I_{AM} is the intensity of the amorphous fraction at 18°.

Thermal properties

The thermal behavior of all the CNC/NCP fomulations was studied by thermogravimetric analysis (TGA), using a Mettler Toledo TGA/SDTA 851e. The films were heated from 25 to 800 °C at a rate of 10 °C min⁻¹ in an inert atmosphere (50 ml min⁻¹ N₂ flow). The ignitions were performed in duplicate for each sample. The data were collected and processed by Mettler-STARE Evaluation software.

The onset, maximum decomposition temperature and mass loss for each thermal decomposition process were obtained. The onset temperature was obtained by extrapolating the slope of the DTG curve corresponding to the first local maximum in D²TG curve down to the zero level of the DTG axis (Yao et al. 2008).

Mechanical properties

The tensile strength of the films was determined with a tensile testing machine (Instron Universal testing machine 5944) fitted with a 250 N load cell. The samples were cut into rectangular test pieces with a width of 5 mm and length of 50 mm, and five replicate specimens were tested for each film type. The initial distance between the grips was 20 mm, and the separation rate of the grips was 2 mm min⁻¹. The stress–strain curve was recorded for each sample. The measurements were performed at 23 °C and 50 % RH, and the tensile data were averaged over five test pieces.

Oxygen-barrier properties

Oxygen permeability measurements were carried out on a Mocon Oxtran 2/20 (Modern Controls Inc., Minneapolis, MN) equipped with a coulometric sensor following ASTM standard D3985-8 (ASTM 2005). Samples were cut into a suitable size and sealed in aluminum foil with a round open area of 5 cm² at atmospheric pressure (760 mmHg). The measurements were conducted at 23 °C, 50 and 80 % RH. Each sample was conditioned at 50 % RH for at least a week followed by 5 h conditioning at the desired test RH in the instrument itself before the measurements began. Two replicates were measured for each sample.

Results and discussion

Film formation

The films prepared from the bark NCP fraction alone were very brittle and fragmented upon drying. The heterogeneity of the matrix, and particularly the presence of Klason lignin (about 4 %), might negatively affect the film formation by e.g. promoting agglomeration of hemicellulose-lignin complexes (Westbye et al. 2007). In order to improve the film

performance, CNCs were introduced into the NCP matrix. Homogeneous transparent films, with a glossy appearance, were obtained when more than 30 wt% CNC was incorporated (Fig. 1). CNCs obviously prevented crack formation and growth, and this resulted in materials with good cohesion.

The topography of the formulations was evaluated by AFM. Representative images of NCP, CNC and the formulations CNC10 and CNC50 are shown in Fig. 2. The surface of the neat CNC film appeared as an interconnected web structure whereas the neat NCP displayed a discontinuous surface with several aggregates. In CNC10, several holes were observed and the cohesion between the CNCs and the NCP seemed rather poor. On the contrary, the CNCs seemed to be totally embedded in the NCP matrix in CNC50. In this formulation, the crystals were randomly orientated, tightly connected to each other, leading to the formation of a continuous network. The differences in topography between CNC10 and CNC50 were in good agreement with the film-forming abilities showed in Fig. 1.

The formulations which gave the best films (a CNC content of 30–50 %) were chosen for the preparation of new films containing sorbitol. The aspect of the plasticized films was similar to the previous films prepared without sorbitol. The influence of sorbitol in terms of structural, thermal, mechanical and morphological properties was subsequently evaluated.

Fourier transform infrared spectrometry (FTIR)

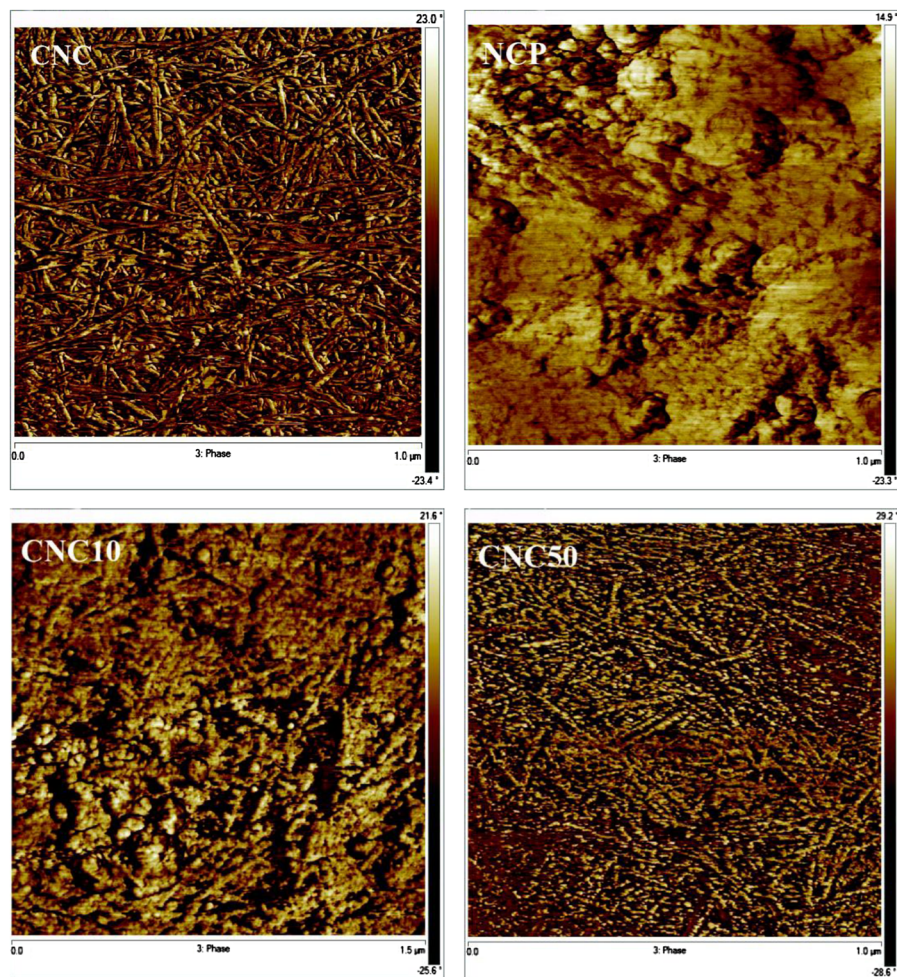
The chemical structures of the CNC, NCP and NCP/CNC formulations were studied by FTIR. The spectra were recorded and the changes in vibrational frequencies of some of the characteristic bands are provided in Online Resource (Figures S1, S2 and Table S1). Four representative spectra are shown in Fig. 3.

The assignment of the characteristic bands of bark components and CNC have already been shown and analyzed in a previous study (Le Normand et al. 2014b). For all the NCP/CNC formulations, the spectra were characterized by a dominant O–H stretching band (3,294–3,322 cm⁻¹) and a C–H stretching band (2,897–2,925 cm⁻¹) corresponding to the aliphatic moieties in the polysaccharides. The top of the band in the O–H stretching region was located at higher wavenumbers for CNC10, CNC20 and CNC30 than for CNC or NCP alone. In contrast,



Fig. 1 Formulations with, from the *left* to the *right*, a CNC content of 10, 20, 30, 40 and 50 %

Fig. 2 AFM images in phase modes of CNC, NCP and the formulations CNC10 and CNC50



the band was shifted to lower wavenumbers when the CNC content was >30 %, indicating an increase in hydrogen bond strength (Kondo 1997; Miya et al. 1984). These observations could be directly related to the film-forming ability of the different formulations. With a CNC content <30 %, the hydrogen interactions between the polysaccharide chains were weak, resulting in cracks. However, when the proportion of CNC was increased to more than 30 %, films with good

cohesion were obtained. When sorbitol was added, the O–H stretching band shifted to even lower wavenumbers, which could be due to an overlap of the sorbitol band ($3,237\text{ cm}^{-1}$) with the CNC and NCP bands.

Wide angle X-ray scattering (WAXS)

The morphology of the NCP/CNC films was investigated using X-ray scattering. Figure 4 shows the

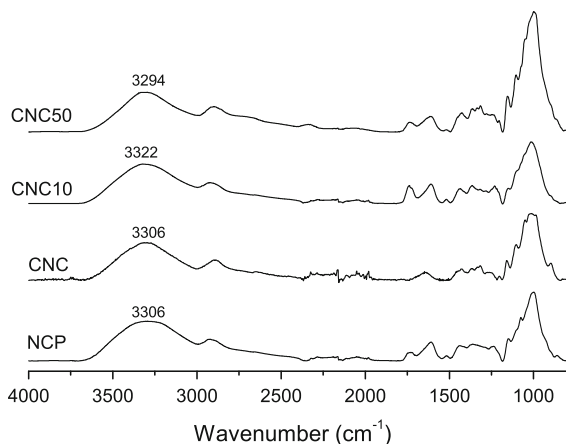


Fig. 3 Selected representative FTIR spectra of NCP, CNC, CNC10 and CNC50

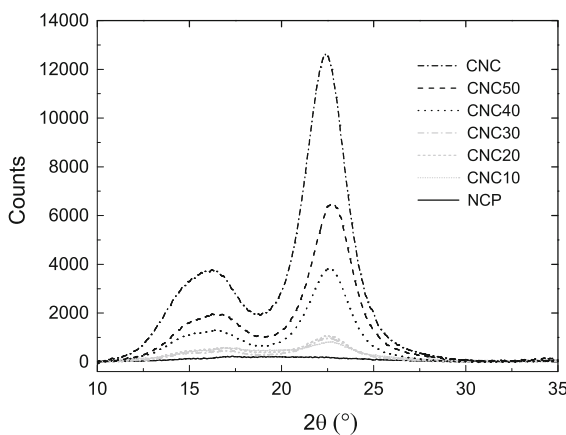


Fig. 4 X-ray diffractograms of NCP, CNC and NCP/CNC films

diffractograms of CNC, NCP and NCP/CNC formulations without plasticizer. CNCs displayed characteristic diffraction peaks at $2\theta = 22.5^\circ$ and 16.2° corresponding to the plane in the sample with the Miller indices (200) and with the contribution of both diffraction peaks (1–10) and (110) at 14.8° and 16.6° , respectively. These peaks were also identified by Le Normand et al., (2014b) and Park et al. (2010). On the other hand, NCP showed a weak and broad peak at $2\theta = 19.5^\circ$.

The NCP/CNC films also displayed two diffraction peaks at 16.2° and 22.5° with different intensities. CNC10, CNC20 and CNC30 exhibited weak and broad diffraction peaks. In contrast, CNC40 and CNC50 showed very distinct diffraction peaks, which suggested that the contribution of CNCs to the overall

Table 1 Crystallinity index (CI) of the NCP/CNC formulations

	CI (%)	
	Without sorbitol	With sorbitol
CNC	84	—
CNC50	85	76
CNC40	83	70
CNC30	71	65
CNC20	63	—
CNC10	45	—

crystallinity of these films was high. The height of the crystalline peak at $2\theta = 22.5^\circ$ was used to compare the relative crystallinities of the films by calculating the CI. The results are summarized in Table 1.

As expected, the CI increased with increasing content of CNC. The crystallinity indices of CNC40 and CNC50 even reached that of CNC alone. This phenomenon was ascribed to an anchoring effect of the CNCs, probably acting as a nucleating agent for the NCP. The starch and pectins contained in the NCP extract probably produce a transcrystalline region around the CNCs. Orientated crystallization of starch on cellulose has already been reported (Anglès and Dufresne 2000; Helbert and Chanzy 1994).

The diffractograms of the NCP/CNC films containing sorbitol were also assessed and the results are provided in Online Resource (Figure S3). The CI of each sorbitol-plasticized film was lower than the value for the unplasticized film with the same CNC content. An explanation could be that the sorbitol intercalated between the NCP and the CNC (Hartman et al. 2006) and therefore reduced the possible interactions between the polysaccharides chains and limited the nucleating behavior of the CNC. The presence of sorbitol in the film resulted in a less ordered system and a decrease in crystallinity.

Thermal properties

The thermal behavior of all the formulations were studied in terms of mass loss, onset temperature and maximum degradation temperatures of the different mass-loss regions, based on the thermogravimetric (TG) and the derivative thermogravimetric (DTG) curves. These thermogravimetric parameters are summarized in Table 2.

Table 2 Thermogravimetric parameters for the thermal degradation of NCP, CNC and NCP/CNC formulations

Samples	25–150 °C		150–600 °C			Residue Mass (%)
	Mass loss (%)	T _{max} (°C)	Onset (°C)	Mass loss (%)	T _{max} (°C)	
NCP	6.3 ± 0.1	63.5 ± 0.2	194.8 ± 0.3	73.2 ± 0.6	253.1 ± 0.6/313.7 ± 0.9	15.0 ± 0.9
CNC10	6.4 ± 0.1	68.1 ± 0.1	216.4 ± 0.3	64.4 ± 0.9	312.1 ± 0.1/345.3 ± 0.5	19.4 ± 1.8
CNC20	5.8 ± 0.1	65.8 ± 1.9	220.4 ± 0.2	69.9 ± 0.2	313.2 ± 2.1/346.2 ± 0.3	20.2 ± 0.3
CNC30	5.2 ± 0.1	70.4 ± 0.1	222.4 ± 0.5	77.5 ± 0.5	321.0 ± 0.6/343.8 ± 0.9	19.4 ± 1.3
CNC40	5.2 ± 0.1	69.8 ± 0.8	227.0 ± 0.2	71.3 ± 5.1	334.3 ± 1.1	18.2 ± 1.4
CNC50	4.9 ± 0.1	68.3 ± 0.1	230.9 ± 0.1	72.8 ± 0.1	331.3 ± 0.4	17.5 ± 1.1
CNC30S	2.3 ± 0.2	83.5 ± 0.4	204.3 ± 0.1	81.1 ± 0.2	309.1 ± 0.1/354.6 ± 0.3	14.9 ± 0.5
CNC40S	2.3 ± 0.2	85.0 ± 1.2	206.1 ± 0.2	84.4 ± 0.5	314.2 ± 0.1/345.3 ± 0.4	13.5 ± 1.2
CNC50S	2.6 ± 0.1	82.2 ± 0.9	210.2 ± 0.5	82.2 ± 0.3	320.2 ± 2.3	16.4 ± 1.0
CNC	4.4 ± 0.2	68.6 ± 0.8	191.5 ± 1.4	64.5 ± 0.1	243.1 ± 0.1/276.9 ± 0.1/356.3 ± 0.1	28.6 ± 0.1

The DTG curves for NCP, CNC and all the formulations are provided in Online Resource (Figure S4)

Figure 5a shows the TG and the DTG curves for CNC, NCP and two of the NCP/CNC formulations (CNC20 and CNC50). The pyrolysis of CNC occurred in three overlapped processes previously assigned to the thermal degradation of the sulfated amorphous region, and the breakdown of the more accessible region and of the least accessible crystal interior (Le Normand et al. 2014b). The thermal degradation of the NCP occurred in two main processes between 200 and 350 °C, where the degradations of pectins and starch usually take place (Liu et al. 2013; Rachini et al. 2009; Stawski 2008). Several mass-loss regions could be observed during the pyrolysis of the NCP/CNC formulations. In the low temperature range (<150 °C), a small mass loss was observed for all the formulations, corresponding to the evaporation of absorbed water, but a slight difference was observed between the formulations with and without sorbitol. In fact, the mass loss due to the evaporation of water (~2 %) from the plasticized films was smaller than that from the unplasticized formulations (~6 %). In addition, the evaporation of water occurred at a higher temperature when sorbitol was added to the matrix, suggesting that unbound water molecules were more trapped within this network. In the high temperature range (150–600 °C), it was possible to distinguish several degradation processes corresponding to the successive degradation of both NCP and CNC. The evolution of the DTG profile of the formulations as a function of the CNC content are provided in Online Resource Figure S4a. For CNC10, CNC20 and CNC30, two distinct degradation processes appeared

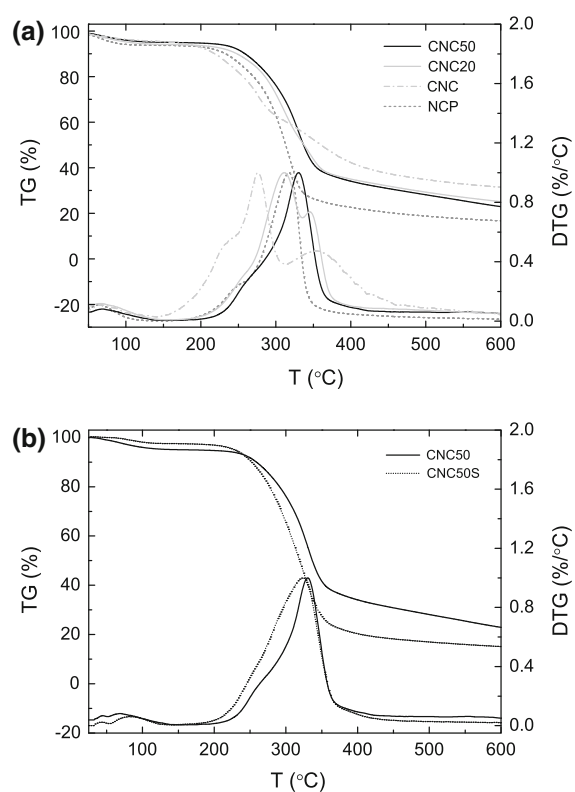


Fig. 5 TG and DTG curves showing **a** the thermal degradation profile of the components alone and in formulations, and **b** the influence of sorbitol on the formulation CNC50

whereas CNC40 and CNC50 showed a more uniform peak on the DTG curve. For the formulation with lower CNC content of 30 % the first T_{max}, around 310–321 °C could clearly be assimilated to the main

Table 3 Tensile properties of NCP/CNC films

	Tensile strength at break (MPa)	Young's modulus (GPa)	Tensile strain at break (%)
CNC50	75.4 ± 5.1	8.2 ± 1.2	0.9 ± 0.3
CNC40	58.4 ± 4.7	8.0 ± 0.4	0.7 ± 0.1
CNC30	22.8 ± 6.5	6.0 ± 1.1	0.3 ± 0.1
CNC50S	79.6 ± 1.6	5.0 ± 0.3	2.6 ± 0.2
CNC40S	62.3 ± 8.0	3.8 ± 0.3	2.2 ± 0.5
CNC30S	60.7 ± 5.6	3.2 ± 0.4	2.5 ± 0.1

degradation peak of the NCP which happens at 313 °C, while the second T_{max} at around 345 °C was most probably due to the degradation of CNC. For CNC40 and CNC50, in which the two components were present in rather equal quantities a narrower and more uniform degradation peak appeared, indicating a more homogeneous material (Figs. 5a, S4a). In contrast, the presence of sorbitol gave a broader degradation peak, indicating a more heterogeneous material (Figs. 5b, S4b).

The temperatures for the onset of thermal degradation of all the formulations were higher than those of the individual components. NCP and CNC started to degrade at around 190 °C whereas the formulations displayed onset temperatures between 205 and 230 °C. Nanocomposite materials with enhanced thermal stability were thus formed by mixing together NCP and CNC. In general, increasing the CNC content led to better thermal stability, but this trend was more significant in the absence of sorbitol (Table 2). The improvement in thermal stability with increasing CNC content could be due to the good intercomponent compatibility and to the increase in crystallinity discussed earlier, but sorbitol seemed to hinder the interactions between NCP and CNC, reducing the crystallinity of the films and their thermal stability.

Mechanical properties

The mechanical properties of the NCP/CNC films were evaluated in term of tensile strength, Young's modulus and tensile strain at break, and the results are summarized in Table 3.

In general, the addition of CNC improved the mechanical properties of the NCP/CNC films. In fact, the tensile strength of the film increased more than three-fold when the CNC content was increased from

30 to 50 %, and the Young's modulus increased from 6.0 to 8.2 GPa. These observations confirmed the presence of strong intermolecular interactions between NCP and CNC, increasing with increasing CNC content. Several authors have reported the same phenomenon and have attributed the improvement in mechanical performance to the percolation mechanism governed by the rigid hydrogen-bonded network of CNCs (Azizi Samir et al. 2005), to the increase in crystalline arrangement in the films (Amash and Zugenmaier 2000; Kaushik et al. 2010; Müller et al. 2009) or to synergic effects between natural components (Mikkonen et al. 2010b). In the case of NCP and CNC, the strong interactions could be due to the presence of highly branched pectins in the extract (Le Normand et al. 2014a) and the natural capability of this polysaccharide to bind to cellulose. In fact, several studies dealing with in vitro adsorption onto cellulose microfibrils of pectins rich in arabinan and galactan side chains showed the ability of pectins to bind to cellulose microfibrils (Zykwinska et al. 2005, 2006, 2007). The strength of the films was comparable to or even better than that of several reported films based on hemicelluloses and CNCs. For instance, films obtained from spruce galactoglucomannan reinforced with 15 % CNC and plasticized with 34 % glycerol had a tensile strength of only 10 MPa (Mikkonen et al. 2010a) while films made from xylan, 10 % CNC and 50 % sorbitol had a tensile strength of <6 MPa (Saxena et al. 2009). The tensile strength of films prepared from starch (Cao et al. 2008) or mango puree (Azeredo et al. 2009) reinforced with CNCs remained close to 9–11 MPa. Moreover, the Young's modulus of the NCP films was much higher than the values obtained for the previously cited polysaccharide films, reported to be between 0.3 and 2.0 GPa. In addition, the tensile strength and Young's modulus of the NCP/CNC films were in the range of those obtained for synthetic polymer materials such as low-density polyethylene, polypropylene, polystyrene and polyvinylchloride (Azeredo et al. 2010).

However, the NCP/CNC films without plasticizer showed very poor flexibility compared with other polysaccharide-based (Azeredo et al. 2009; Cao et al. 2008; Mikkonen et al. 2010a; Saxena et al. 2009) or synthetic films (Azeredo et al. 2010). In fact, the elongation of the films was <1 %, which indicated a very brittle material. The addition of sorbitol was expected to improve this property.

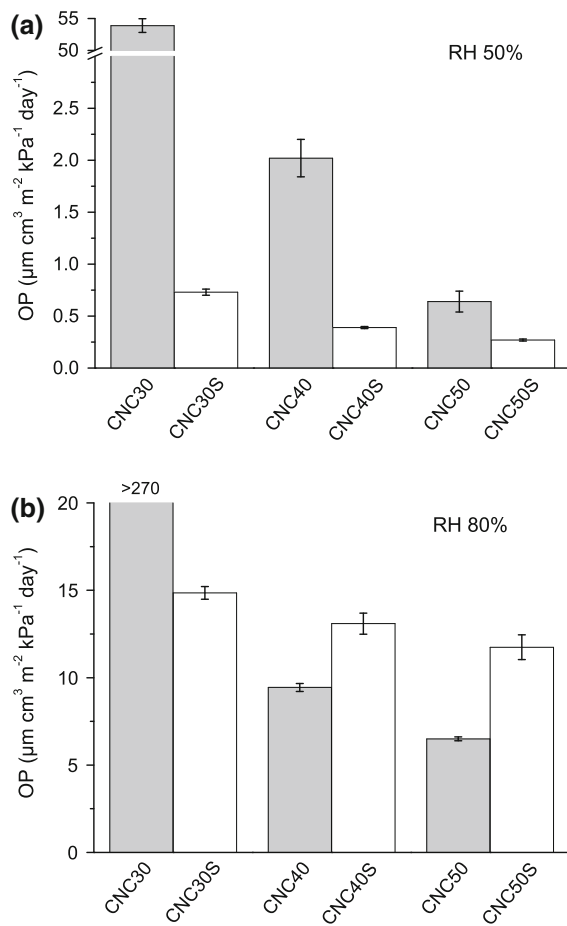


Fig. 6 Effect of the addition of CNC and sorbitol on the oxygen permeability (OP) of the NCP/CNC films at **a** 50 % RH and **b** 80 % RH

In general, the Young's modulus of the films decreased when sorbitol was added, resulting in a less stiff material. On the other hand, the strength of the films remained unchanged when sorbitol was added to CNC40 and CNC50, whereas it was improved by 270 % for CNC30. The behavior of CNC30/CNC30S was probably related to the weaknesses of CNC30 in term of cohesion, leading to a greater contribution of the sorbitol as a plasticizer in this particular case. The most obvious mechanical improvement in the presence of sorbitol was the flexibility. In fact, the addition of sorbitol significantly increased the flexibility of all the films more than threefold. Similar elongation values were reached for all the plasticized films. It was not therefore possible to observe a clear contribution of CNC in these cases.

Oxygen-barrier properties

In the previous sections, the addition of CNCs was shown to increase the intermolecular interactions in the matrix. This strong network was therefore expected to offer a high oxygen-barrier. In food packaging, high oxygen-barrier performance is usually related to an OP of $<39 \mu\text{m}^3 \text{m}^{-2} \text{kPa}^{-1} \text{day}^{-1}$. As seen in Fig. 6, the oxygen permeabilities of most of the films met this criterion at both 50 % RH and 80 % RH. The only film that provided a very poor oxygen-barrier was CNC30. The reason for its high permeability may be due to the fragility, low crystallinity, difficulty to handle and rather low molecular interactions between the components, which were pointed out earlier.

In general, the addition of CNC to the matrix significantly improved the oxygen-barrier performance of all the NCP/CNC films at both 50 % RH and 80 % RH. When the CNC content was increased from 30 to 50 %, the OP of the films at 50 % RH was considerably lowered from 54 to $0.64 \mu\text{m}^3 \text{m}^{-2} \text{kPa}^{-1} \text{day}^{-1}$. The addition of sorbitol further improved the barrier properties of the NCP/CNC films at 50 % RH. Considering all the films prepared in this study, the best oxygen-barrier performance at 50 % RH was achieved with the CNC50 film with 30 % sorbitol ($0.27 \mu\text{m}^3 \text{m}^{-2} \text{kPa}^{-1} \text{day}^{-1}$).

All the films showed a higher permeability at 80 % than 50 % RH, which was expected, considering the hydrophilic nature of polysaccharides. It is well-known that, as soon as the humidity increases, polysaccharides tend to absorb moisture and this leads to a swelling of the films and a subsequent increase in gas permeability (Kochumalayil and Berglund 2014; Yaich et al. 2014). At 80 % RH, the best performance was obtained with CNC50, which had an OP of $6.5 \mu\text{m}^3 \text{m}^{-2} \text{kPa}^{-1} \text{day}^{-1}$. The high barrier performance of CNC50 could be due to the strong interactions in the matrix described earlier, and also to the high crystallinity of the material. In fact, high crystallinity is often associated with low permeability (Lagaron et al. 2004; McGonigle et al. 2001).

The addition of sorbitol had an effect at 80 % RH contrary to that at 50 % RH. In fact, the presence of sorbitol significantly reduced the barrier performance of the films at 80 %, probably due to the softener behavior of sorbitol at high RH. Hartman et al. (2006) reported that films made from spruce AcGGM with

Table 4 Oxygen permeability (OP) of some polysaccharide-based films and commercial materials

	Other components	OP ($\mu\text{m cm}^3 \text{ m}^{-2} \text{ kPa}^{-1} \text{ day}^{-1}$)	RH	References
<i>Polysaccharide-based films</i>				
Spruce bark NCP (this study)	50 % CNC/30 % sorbitol ^a	0.27	50	This study
Spruce bark NCP (this study)	50 % CNC	6.5	80	This study
Arabinoglucuronoxylan from Norway spruce		0.12	50	Escalante et al. (2012)
Arabinoxylan from Oat spelt	50 % CNC	0.13	50	Saxena et al. (2010)
Arabinoxylan from Norway spruce	25 % sorbitol	0.17	50	Escalante et al. (2012)
Glucuronoxylan from Aspen wood	35 % sorbitol	0.21	50	Gröndahl et al. (2004)
Galactoglucomannan-rich wood hydrolysate	50 % CMC	0.3	50	Edlund et al. (2010)
AcGGM	35 % CMC	1.28	50	Hartman et al. (2006)
AcGGM	35 % sorbitol	2.0	50	Hartman et al. (2006)
Arabinoxylan from Oat spelt	40 % sorbitol	4.7	50–75	Mikkonen et al. (2009)
Konjac glucomannan	5 % CNC/40 % sorbitol	5	50–75	Mikkonen et al. (2010b)
AcGGM	40 % sorbitol	6.8	50–75	Mikkonen et al. (2010b)
<i>Commercial films</i>				
Polyvinylidene chloride (PVDC)		0.1–3	50	Lange and Wyser (2003)
Polyvinylalcohol (PVOH)		0.21	50	Gröndahl et al. (2004)
Ethylene vinyl alcohol (EVOH)		0.3	50	Hansen and Plackett (2008)
Polyethylene-terephthalate (PET)		14.6	50	Ryberg et al. (2011)
Polyethylene-terephthalate (PET)		15.7	80	Ryberg et al. (2011)
Polyvinyl chloride (PVC)		20–80	50	Lange and Wyser (2003)
Polylactic acid (PLA)		160	50	Hansen and Plackett (2008)
Polypropylene (PP)		500–1,000	50	Lange and Wyser (2003)
Polyethylene (PE)		500–2,000	50	Lange and Wyser (2003)
Polystyrene (PS)		1,000–1,500	50	Lange and Wyser (2003)

^a The sorbitol content is indicated on the basis of the dry polysaccharide weight

sorbitol softened markedly at a humidity higher than 70 % RH.

The OP of bark NCP/CNC films was compared to the values obtained for several polysaccharide-based films and commercial polymers (Table 4). The OP of the NCP/CNC films was comparable to or lower than the values reported for films obtained from xylan, starch, glucomannan and mixtures of various polysaccharides, and the OPs of NCP/CNC films were much lower than the values reported for e.g. polylactic acid, polyvinyl chloride and polyethylene-terephthalate which are extensively used in packaging applications.

Conclusion

The NCP fraction obtained by hot-water extraction of spruce bark was found to be an excellent candidate for making renewable nanocomposites. It was necessary to add CNC in order to improve the mechanical, thermal and oxygen-barrier properties of the films. These properties could be tailored by varying the quantities of CNC and sorbitol added to the NCP matrix. On the one hand, the addition of the CNC resulted in an improvement in the thermal, mechanical and oxygen-barrier performances of the films due to

the strong hydrogen-bond interactions between the NCP and the CNC. On the other hand, the addition of sorbitol allowed the formation of films with better flexibility and lower OP at 50 % RH. However, the presence of plasticizer in the NCP/CNC films made the film more susceptible to moisture and reduced the oxygen-barrier performance at 80 % RH. The quantities of CNCs and sorbitol must be carefully chosen in order to meet the criteria for the final application. Since all the raw materials used for the nanocomposite preparation could be obtained from bark, this work strongly supported the bark biorefinery concept.

Acknowledgments This work was supported by the Wood Wisdom ERA-NET Program (WOBAMA Project) and by the VINNOVA and Ångpanneföreningens Forskningsstiftelse funding agencies (Myriam Le Normand). The authors acknowledge the Wallenberg and Lars-Erik Thunholm Foundation for the post-doctoral research position granted to Rosana Moriana.

References

- Amash A, Zugenmaier P (2000) Morphology and properties of isotropic and oriented samples of cellulose fibre–polypropylene composites. *Polymer* 41:1589–1596. doi:[10.1016/S0032-3861\(99\)00273-6](https://doi.org/10.1016/S0032-3861(99)00273-6)
- Anglès MN, Dufresne A (2000) Plasticized starch/tunicin whiskers nanocomposites. 1. Structural analysis. *Macromolecules* 33:8344–8353. doi:[10.1021/ma0008701](https://doi.org/10.1021/ma0008701)
- ASTM (2005) ASTM D3985-05 standard test method for oxygen gas transmission rate through plastic film and sheeting using a coulometric sensor. ASTM International, West Conshohocken
- Azeredo HMC, Mattoso LHC, Wood D, Williams TG, Avena-Bustillos RJ, McHugh TH (2009) Nanocomposite edible films from mango puree reinforced with cellulose nanofibers. *J Food Sci* 74:N31–N35. doi:[10.1111/j.1750-3841.2009.01186.x](https://doi.org/10.1111/j.1750-3841.2009.01186.x)
- Azeredo HMC, Mattoso LHC, Avena-Bustillos RJ, Filho GC, Munford ML, Wood D, McHugh TH (2010) Nanocellulose reinforced chitosan composite films as affected by nano-filler loading and plasticizer content. *J Food Sci* 75:N1–N7. doi:[10.1111/j.1750-3841.2009.01386.x](https://doi.org/10.1111/j.1750-3841.2009.01386.x)
- Azizi Samir MAS, Alloin F, Dufresne A (2005) Review of recent research into cellulosic whiskers, their properties and their application in nanocomposite field. *Biomacromolecules* 6:612–626. doi:[10.1021/bm0493685](https://doi.org/10.1021/bm0493685)
- Bertaud F, Holmbom B (2004) Chemical composition of earlywood and latewood in Norway spruce heartwood, sapwood and transition zone wood. *Wood Sci Technol* 38:245–256. doi:[10.1007/s00226-004-0241-9](https://doi.org/10.1007/s00226-004-0241-9)
- Cao X, Chen Y, Chang PR, Stumborg M, Huneault MA (2008) Green composites reinforced with hemp nanocrystals in plasticized starch. *J Appl Polym Sci* 109:3804–3810. doi:[10.1002/app.28418](https://doi.org/10.1002/app.28418)
- Co M, Fagerlund A, Engman L, Sunnerheim K, Sjöberg PJR, Turner C (2012) Extraction of antioxidants from spruce (*Picea abies*) bark using eco-friendly solvents. *Phytochem Anal* 23:1–12. doi:[10.1002/pca.1316](https://doi.org/10.1002/pca.1316)
- Dufresne A (2008) Polysaccharide nano crystal reinforced nanocomposites. *Can J Chem* 86:484–494. doi:[10.1139/v07-152](https://doi.org/10.1139/v07-152)
- Edlund U, Ryberg YZ, Albertsson A-C (2010) Barrier films from renewable forestry waste. *Biomacromolecules* 11:2532–2538
- Escalante A, Gonçalves A, Bodin A, Stepan A, Sandström C, Toriz G, Gatenholm P (2012) Flexible oxygen barrier films from spruce xylan. *Carbohydr Polym* 87:2381–2387. doi:[10.1016/j.carbpol.2011.11.003](https://doi.org/10.1016/j.carbpol.2011.11.003)
- Gröndahl M, Eriksson L, Gatenholm P (2004) Material properties of plasticized hardwood xyans for potential application as oxygen barrier films. *Biomacromolecules* 5:1528–1535. doi:[10.1021/bm049925n](https://doi.org/10.1021/bm049925n)
- Hansen NML, Plackett D (2008) Sustainable films and coatings from hemicelluloses: a review. *Biomacromolecules* 9:1493–1505. doi:[10.1021/bm000053z](https://doi.org/10.1021/bm000053z)
- Hartman J, Albertsson A-C, Lindblad MS, Sjöberg J (2006) Oxygen barrier materials from renewable sources: material properties of softwood hemicellulose-based films. *J Appl Polym Sci* 100:2985–2991
- Helbert W, Chanzy H (1994) Oriented growth of V amylose n-butanol crystals on cellulose. *Carbohydr Polym* 24:119–122. doi:[10.1016/0144-8617\(94\)90021-3](https://doi.org/10.1016/0144-8617(94)90021-3)
- Ibn Yaich A, Edlund U, Albertsson A-C (2011) Wood hydrolysate barriers: performance controlled via selective recovery. *Biomacromolecules* 13:466–473. doi:[10.1021/bm201518d](https://doi.org/10.1021/bm201518d)
- Kaushik A, Singh M, Verma G (2010) Green nanocomposites based on thermoplastic starch and steam exploded cellulose nanofibrils from wheat straw. *Carbohydr Polym* 82:337–345. doi:[10.1016/j.carbpol.2010.04.063](https://doi.org/10.1016/j.carbpol.2010.04.063)
- Kemppainen K, Siika-aho M, Pattathil S, Giovando S, Kruus K (2014) Spruce bark as an industrial source of condensed tannins and non-cellulosic sugars. *Ind Crop Prod* 52:158–168. doi:[10.1016/j.indcrop.2013.10.009](https://doi.org/10.1016/j.indcrop.2013.10.009)
- Kochumalayil JJ, Berglund LA (2014) Water-soluble hemicelluloses for high humidity applications—enzymatic modification of xyloglucan for mechanical and oxygen barrier properties. *Green Chem* 16:1904–1910. doi:[10.1039/c3gc41823e](https://doi.org/10.1039/c3gc41823e)
- Kondo T (1997) The assignment of IR absorption bands due to free hydroxyl groups in cellulose. *Cellulose* 4:281–292. doi:[10.1023/a:1018448109214](https://doi.org/10.1023/a:1018448109214)
- Krogell J, Holmbom B, Pranovich A, Hemming J, Willför S (2012) Extraction and chemical characterization of Norway spruce inner and outer bark. *Nord Pulp Pap Res J* 27:6–17
- Lagaron JM, Catalá R, Gavara R (2004) Structural characteristics defining high barrier properties in polymeric materials. *Mater Sci Technol* 20:1–7. doi:[10.1179/026708304225010442](https://doi.org/10.1179/026708304225010442)
- Lange J, Wyser Y (2003) Recent innovations in barrier technologies for plastic packaging—a review. *Packag Technol Sci* 16:149–158. doi:[10.1002/pts.621](https://doi.org/10.1002/pts.621)
- Le Normand M, Edlund U, Holmbom B, Ek M (2012) Hot-water extraction and characterization of spruce bark non-cellulosic polysaccharides. *Nord Pulp Pap Res J* 27:18–23

- Le Normand M et al (2014a) Hot-water extracts from the inner bark of Norway spruce with immunomodulating activities. *Carbohydr Polym* 101:699–704. doi:[10.1016/j.carbpol.2013.09.067](https://doi.org/10.1016/j.carbpol.2013.09.067)
- Le Normand M, Moriana R, Ek M (2014b) Isolation and characterization of cellulose nanocrystals from spruce bark in a biorefinery perspective. *Carbohydr Polym* 111:979–987. doi:[10.1007/s10570-014-0423-z](https://doi.org/10.1007/s10570-014-0423-z)
- Liu X, Wang Y, Yu L, Tong Z, Chen L, Liu H, Li X (2013) Thermal degradation and stability of starch under different processing conditions. *Starch–Stärke* 65:48–60. doi:[10.1002/star.201200198](https://doi.org/10.1002/star.201200198)
- Mariano M, El Kissi N, Dufresne A (2014) Cellulose nanocrystals and related nanocomposites: review of some properties and challenges. *J Polym Sci, Part B: Polym Phys* 52:791–806. doi:[10.1002/polb.23490](https://doi.org/10.1002/polb.23490)
- McGonigle EA, Liggett JJ, Pethrick RA, Jenkins SD, Daly JH, Hayward D (2001) Permeability of N₂, Ar, He, O₂ and CO₂ through biaxially oriented polyester films—dependence on free volume. *Polymer* 42:2413–2426. doi:[10.1016/S0032-3861\(00\)00615-7](https://doi.org/10.1016/S0032-3861(00)00615-7)
- Mikkonen KS et al (2009) Films from oat spelt arabinoxylan plasticized with glycerol and sorbitol. *J Appl Polym Sci* 114:457–466. doi:[10.1002/app.30513](https://doi.org/10.1002/app.30513)
- Mikkonen K et al (2010a) Glucomannan composite films with cellulose nanowhiskers. *Cellulose* 17:69–81. doi:[10.1007/s10570-009-9380-3](https://doi.org/10.1007/s10570-009-9380-3)
- Mikkonen KS, Heikkilä MI, Helén H, Hyvönen L, Tenkanen M (2010b) Spruce galactoglucomanan films show promising barrier properties. *Carbohydr Polym* 79:1107–1112. doi:[10.1016/j.carbpol.2009.10.049](https://doi.org/10.1016/j.carbpol.2009.10.049)
- Miranda I, Gominho J, Mirra I, Pereira H (2012) Chemical characterization of barks from *Picea abies* and *Pinus sylvestris* after fractioning into different particle sizes. *Ind Crop Prod* 36:395–400. doi:[10.1016/j.indcrop.2011.10.035](https://doi.org/10.1016/j.indcrop.2011.10.035)
- Miya M, Iwamoto R, Mima S (1984) FT-IR study of intermolecular interactions in polymer blends. *J Polym Sci: Polym Phys Ed* 22:1149–1151. doi:[10.1002/pol.1984.180220615](https://doi.org/10.1002/pol.1984.180220615)
- Moriana R, Vilaplana F, Karlsson S, Ribes-Greus A (2011) Improved thermo-mechanical properties by the addition of natural fibres in starch-based sustainable biocomposites. *Compos Part A: Appl Sci Manuf* 42(1):30–40. doi:[10.1016/j.compositesa.2010.10.001](https://doi.org/10.1016/j.compositesa.2010.10.001)
- Müller CMO, Laurindo JB, Yamashita F (2009) Effect of cellulose fibers on the crystallinity and mechanical properties of starch-based films at different relative humidity values. *Carbohydr Polym* 77:293–299. doi:[10.1016/j.carbpol.2008.12.030](https://doi.org/10.1016/j.carbpol.2008.12.030)
- Nilsson K, Sangster M, Gallis C, Hartig T, de Vries S, Seeland K, Schipperijn J (2011) Forests, trees and human health. Springer, Dordrecht
- Park S, Baker J, Himmel M, Parilla P, Johnson D (2010) Cellulose crystallinity index: measurement techniques and their impact on interpreting cellulase performance. *Biootechnol Biofuels* 3:10
- Pietarinen S, Willför S, Ahotupa M, Hemming J, Holmbom B (2006) Knotwood and bark extracts: strong antioxidants from waste materials. *J Wood Sci* 52:436–444. doi:[10.1007/s10086-005-0780-1](https://doi.org/10.1007/s10086-005-0780-1)
- Pizzi A (2006) Recent developments in eco-efficient bio-based adhesives for wood bonding: opportunities and issues. *J Adhes Sci Technol* 20:829–846. doi:[10.1163/156856106777638635](https://doi.org/10.1163/156856106777638635)
- Rachini A, Le Troedec M, Peyratout C, Smith A (2009) Comparison of the thermal degradation of natural, alkali-treated and silane-treated hemp fibers under air and an inert atmosphere. *J Appl Polym Sci* 112:226–234. doi:[10.1002/app.29412](https://doi.org/10.1002/app.29412)
- Ragauskas AJ et al (2006) The path forward for biofuels and biomaterials. *Science* 311:484–489. doi:[10.1126/science.1114736](https://doi.org/10.1126/science.1114736)
- Ryberg ZYZ, Edlund U, Albertsson AC (2011) Conceptual approach to renewable barrier film design based on wood hydrolysate. *Biomacromolecules* 12:1355–1362. doi:[10.1021/bm200128s](https://doi.org/10.1021/bm200128s)
- Saxena A, Elder TJ, Pan S, Ragauskas AJ (2009) Novel nanocellulosic xylan composite film. *Compos Part B: Eng* 40:727–730. doi:[10.1016/j.compositesb.2009.05.003](https://doi.org/10.1016/j.compositesb.2009.05.003)
- Saxena A, Elder T, Kenvin J, Ragauskas A (2010) High oxygen nanocomposite barrier films based on xylan and nanocrystalline cellulose. *Nano–Micro Lett* 2:235–241. doi:[10.3786/nml.v2i4](https://doi.org/10.3786/nml.v2i4)
- Segal L, Creely JJ, Martin AE, Conrad CM (1959) An empirical method for estimating the degree of crystallinity of native cellulose using the X-ray diffractometer. *Text Res J* 29:786–794. doi:[10.1177/004051755902901003](https://doi.org/10.1177/004051755902901003)
- Shen L, Patel M (2008) Life cycle assessment of polysaccharide materials: a review. *J Polym Environ* 16:154–167. doi:[10.1007/s10924-008-0092-9](https://doi.org/10.1007/s10924-008-0092-9)
- Stawski D (2008) New determination method of amylose content in potato starch. *Food Chem* 110:777–781. doi:[10.1016/j.foodchem.2008.03.009](https://doi.org/10.1016/j.foodchem.2008.03.009)
- Westbye P, Köhnke T, Glasser W, Gatenholm P (2007) The influence of lignin on the self-assembly behaviour of xylan rich fractions from birch (*Betula pendula*). *Cellulose* 14:603–613. doi:[10.1007/s10570-007-9178-0](https://doi.org/10.1007/s10570-007-9178-0)
- Yaich AI, Edlund U, Albertsson A-C (2014) Adapting wood hydrolysate barriers to high humidity conditions. *Carbohydr Polym* 100:135–142. doi:[10.1016/j.carbpol.2012.10.079](https://doi.org/10.1016/j.carbpol.2012.10.079)
- Yao F, Wu Q, Lei Y, Guo W, Xu Y (2008) Thermal decomposition kinetics of natural fibers: activation energy with dynamic thermogravimetric analysis. *Polym Degrad Stab* 93:90–98. doi:[10.1016/j.polymdegradstab.2007.10.012](https://doi.org/10.1016/j.polymdegradstab.2007.10.012)
- Zykwinska AW, Ralet MC, Garnier CD, Thibault JF (2005) Evidence for in vitro binding of pectin side chains to cellulose. *Plant Physiol* 139:397–407
- Zykwinska A, Gaillard C, Buléon A, Pontoire B, Garnier C, Thibault J-F, Ralet M-C (2006) Assessment of in vitro binding of isolated pectic domains to cellulose by adsorption isotherms, electron microscopy, and X-ray diffraction methods. *Biomacromolecules* 8:223–232. doi:[10.1021/bm060292h](https://doi.org/10.1021/bm060292h)
- Zykwinska A, Thibault JF, Ralet MC (2007) Organization of pectic arabinan and galactan side chains in association with cellulose microfibrils in primary cell walls and related models envisaged. *J Exp Bot* 58:1795–1802